



Published in final edited form as:

J Bone Miner Res. 2014 July ; 29(7): 1564–1574. doi:10.1002/jbmr.2275.

Core binding factor beta (*Cbfb*) controls the balance of chondrocyte proliferation and differentiation by up-regulating Indian hedgehog (*Ihh*) expression and inhibiting parathyroid hormone-related protein Receptor (PPR) expression in postnatal cartilage and bone formation

Fei Tian^{#1,2}, Mengrui Wu^{#2,3}, Lianfu Deng¹, Guochun Zhu², Junqing Ma², Bo Gao², Lin Wang⁴, Yi-Ping Li^{#2}, and Wei Chen^{#2}

¹Shanghai Institute of Traumatology and Orthopedics, Ruijin Hospital, Jiao Tong University School of Medicine, Shanghai 200025, People's Republic of China.

²Department of Pathology, University of Alabama at Birmingham, USA.

³Institute of Genetics, Life Science College, Zhejiang University, People's Republic of China.

⁴Institute of Stomatology, Nanjing Medical University, 140 Hangzhou Road, Nanjing, Jiangsu 210029, China. USA.

These authors contributed equally to this work.

Abstract

Core binding factor beta (*Cbfb*) is essential for embryonic bone morphogenesis. Yet, the mechanisms by which *Cbfb* regulates chondrocyte proliferation and differentiation as well as postnatal cartilage and bone formation remain unclear. Hence, using the *paired-related homeobox transcription factor 1*-Cre (*Prx1*-Cre) mice, mesenchymal stem cell-specific *Cbfb*-deficient (*Cbfb*^{fl/fl} *Prx1*-Cre) mice were generated to study the role of *Cbfb* in postnatal cartilage and bone development. These mutant mice survived to adulthood but exhibited severe sternum and limb malformations. Sternum ossification was largely delayed in the *Cbfb*^{fl/fl} *Prx1*-Cre mice and the xiphoid process was non-calcified and enlarged. In newborn and 7-day-old *Cbfb*^{fl/fl} *Prx1*-Cre mice, the resting zone was dramatically elongated, the proliferation zone and hypertrophic zone of the growth plates were drastically shortened and disorganized, and trabecular bone formation was reduced. Moreover, in one-month-old *Cbfb*^{fl/fl} *Prx1*-Cre mice, the growth plates were severely deformed and trabecular bone was almost absent. In addition, *Cbfb* deficiency impaired

#Address of Corresponding author: Wei Chen, MD: Department of Pathology, University of Alabama at Birmingham, SHEL 815, 1825 University Blvd, Birmingham, AL 35294, USA, Tel: 205.975.2605, Fax: 205.975.4919, wechen@uab.edu or Yi-Ping Li, PhD: Department of Pathology, University of Alabama at Birmingham, SHEL 810, 1825 University Blvd, Birmingham, AL 35294, USA, Tel: 205.975.2606, Fax: 205.975.4919, ypli@uab.edu.

Additional Supporting Information may be found in the online version of this article.

Disclosures

All authors state that they have no conflicts of interest.

Authors' roles: Study design: YPL and WC. Study conduct: FT, MW, WC, JM, GZ, BG. Data collection and analysis: MW, FT, WC, LD, JM, GZ, BG, LW and YPL. Drafting manuscript: MW, WC, FT and YPL. Revising manuscript: MW, WC and YPL. All authors approved the final version of the manuscript for submission. WC and YPL take responsibility for the integrity of data analysis.

intramembranous bone formation both *in vivo* and *in vitro*. Interestingly, while the expression of Indian hedgehog (Ihh) was largely reduced, the expression of Parathyroid hormone-related protein (PTHrP) receptor (PPR) was dramatically increased in the *Cbfb^{f/f}Prx1*-Cre growth plate, indicating that *Cbfb* deficiency disrupted the Ihh-PTHrP negative regulatory loop. Chromatin immunoprecipitation (ChIP) analysis and promoter luciferase assay demonstrated that the Runx/Cbfb complex binds putative Runx-binding sites of the *Ihh* promoter regions, and also Runx/Cbfb complex directly up-regulates *Ihh* expression at the transcriptional level. Consistently, the expressions of Ihh target genes, including *CyclinD1*, *Ptc* and *Pthlh*, were down-regulated in *Cbfb*-deficient chondrocytes. Taken together, our study reveals not only that Cbfb is essential for chondrocyte proliferation and differentiation for the growth and maintenance of the skeleton in postnatal mice, but also that it functions in up-regulating Ihh expression to promoter chondrocyte proliferation and osteoblast differentiation and inhibiting PPR expression to enhance chondrocyte differentiation.

Keywords

genetic animal models; signaling pathways; development; osteoblasts; growth plate; Indian hedgehog

Introduction

Core binding factors (CBFs) are heterodimeric transcription factors composed of two subunits: the core binding factor alpha (CBF α) and core binding factor beta (CBF β) (1). CBF α subunits are encoded by three gene, namely, *Runt-related transcription factor 1* (*Runx1*) (*Cbfa2*), *Runx2* (*Cbfa1*) and *Runx3* (*Cbfa3*) (2), each of which plays important roles in skeletal development. Runx2 is a key transcription factor associated with osteoblast differentiation and chondrocyte hypertrophy (3), Runx3 is indispensable for endochondral ossification if the *Runx2* gene dosage is reduced (4), and Runx1 cooperates with Runx2 to regulate sternal morphogenesis (5,6). The non-DNA-binding subunit, Cbfb, cooperates with Cbfa to form DNA-protein complexes and protects the Cbfa subunits from degradation (7). *Cbfb*^{-/-} embryos died from an absence of fetal liver hematopoiesis at mid-gestation (8,9). This barrier had impeded further research in understanding the role of Cbfb in skeletal development until the generation of the three mice models (*Cbfb*^{GFP/GFP} knock-in mice, and *Tek*-GFP/*Cbfb* and *Gata1*-*Cbfb* transgenic mice) in 2002 (10-12). *Cbfb*^{GFP/GFP} knock-in mice died soon after birth. *Cbfb*^{-/-} embryos that were rescued by *Tek*-GFP/*Cbfb* [*Cbfb*^{-/-}-Tg(*Tek*-GFP/*Cbfb*)] and *Gata1*-*Cbfb* [*Cbfb*^{-/-}-Tg(*Gata1*-*Cbfb*)] transgene died around birth. These mouse models enabled the study of Cbfb's role in embryonic skeletal development (10-12). The role of *Cbfb* in postnatal bone formation was unexplored until the generation of *Cbfb*/*Runx2* double transgenic mice, which exhibited severe osteopenia (13). However, the physiological defects caused by *Cbfb* deficiency in postnatal mice have not yet been clarified. To further explore the role of Cbfb in skeletal development, we generated mesenchymal stem cell (MSC)-specific *Cbfb* conditional knockout mice by crossing *Cbfb*^{f/f} mice (14) with (*paired-related homeobox transcription factor 1*) *Prx1*-Cre mice (15). Cre expression driven by the *Prx1*-promoter was first detected in the forelimb mesenchyme at embryonic day (E) 9.5 and then in all MSCs at E10.5 (15). *Cbfb*^{f/f}*Prx1*-Cre mice survived

into adulthood, *Cbfb^{f/f}Prx1-Cre* mice displayed short limbs, short statures, inhibited osteoblastogenesis, inhibited chondrocyte differentiation, and impaired trabeculae formation. In addition, Cyclin D1, Indian hedgehog (Ihh) and parathyroid hormone-related protein receptor (PPR) expression were dysregulated in the growth plates of the *Cbfb^{f/f}Prx1-Cre* mice.

Materials and Methods

Generation of *Cbfb* conditional knockout mice

Cbfb^{f/f} mice (B6.129P2-*Cbfb^{tm1Itan/J}*) mice (14) and *Prx1-Cre* (B6.Cg-Tg(*Prx1-Cre*)1Cjt/J) (15) (Jackson Laboratory) were crossed to generate *Cbfb^{f/+}Prx1-cre* mice, and their progeny were intercrossed to obtain *Cbfb^{f/f}Prx1-cre* mice. Mice were housed in the animal room of University of Alabama at Birmingham (UAB) (Birmingham, AL, USA). All research procedures using mice were approved by the UAB Animal Care and Use Committee and conformed to NIH guidelines.

Statistical analysis and data quantification analysis

All data were presented as the mean \pm standard deviation (SD). Statistical significance was assessed using Student's t-test performed with the SPSS 16.0 software (SPSS Incorporation, Chicago, IL, USA). P-values <0.05 were considered significant, and labeled * $p<0.05$, ** $p<0.01$, *** $p<0.001$ in the graphs. The results are representative of at least six individual experiments ($n\geq 6$).

Results

Spatial and temporal expression of *Cbfb* in wild-type (WT) mouse skeleton

Expression of *Cbfb* in skeletons at postnatal one-day-old (P1) mice was detected by immunohistochemistry (IHC) using paraffin sections. The results showed that *Cbfb* is highly expressed in proliferative chondrocytes, hypertrophic chondrocytes, and osteoblasts in long bones (Supplementary Fig. S1A), vertebrae (Supplementary Fig. S1B), and ribs (Supplementary Fig. S1C).

MSC-specific *Cbfb*-deficient mice exhibited dwarfism with skeletal malformation and delayed ossification

MSC-specific *Cbfb*-deficient mice were generated by crossing *Cbfb^{f/f}* mice with *Prx1-cre* mice, and genotypes were confirmed by PCR analysis (Fig. 1L). Efficient ablation of *Cbfb* expression in chondrocytes and osteoblasts in ribs, vertebrae, and long bones in *Cbfb^{f/f}Prx1-Cre* mice was confirmed by IHC (Supplementary Fig. S2A-C). Although a small portion (~10%) of homozygotes died of asphyxiation problems soon after birth, most survived into adulthood. Male homozygotes were fertile. Female homozygotes were able to conceive, although dystocia would occur, probably due to an abnormal pelvis (Fig. 2A, upper panel and lower panel). Postnatal seven-day-old (P7) *Cbfb^{f/f}Prx1-Cre* mice exhibited dwarfism (Fig. 1A, B) with shortened limbs (Fig. 1A-D) compared to WT cohorts. Bone morphology of P7 mice was analysed by Alizarin red S/Alcian blue staining (Fig. 1B-I). Although limbs were shortened, the epiphyseal cartilage (blue color) was elongated (Fig. 1C,D) in the

Cbfb^{fl/fl}Prx1-Cre mice. In addition, mutant mice had widened sutures and enlarged fontanelles, with delayed ossification of the parietal and frontal bones (Fig. 1F). Ossification of the sternum (Fig. 1H) and hyoid bone (Fig. 1I) were also delayed in mutant mice compared to WT mice. The xiphoid process was non-calcified and abnormally enlarged (Fig. 1H). Spines and ribs didn't show notable morphological changes in P7 mutant mice (Fig. 1E, G), but they did show delayed ossification in P1 mutant mice (Supplementary Fig. S2D, E). Thus, defects may be compensated for as the mice aged. Finally, the short-limb deformity observed in the mutant mice (Fig. 1A-D) persists with age, which was confirmed again by Alizarin red S/Alcian blue (Fig. 1J) and micro-CT analysis (Fig. 1K) of one-month-old (P30) mice. Notably, X-ray analysis showed that six-week-old *Cbfb^{fl/fl}Prx1-Cre* mice displayed several characteristics of cleidocranial dysplasia (e.g. short stature, short limb, and absent clavicles) (Fig. 2A). Taken together, these results indicate that loss of *Cbfb* results in dwarfism, limb and sternum malformation, and delayed skeletal ossification during postnatal skeletal development.

Loss of *Cbfb* impaired skeletal development in newborn mice

Next, to examine the role of *Cbfb* in the differentiation of chondrocytes, osteoblasts, and osteoclasts in newborn mice, hematoxylin and eosin (H&E) staining, Safranin O staining, Goldner's trichrome staining, and TRAP staining were performed on paraffin sections of femurs (Fig. 2B-F). Compared with WT mice, newborn *Cbfb^{fl/fl}Prx1-Cre* mice had elongated growth plates and shortened diaphysis (Fig. 2B, C). Although the resting zone was elongated, the proliferation zone was shortened and the proliferative columns, which were presented in the WT growth plates, were disrupted in newborn mutant mice (Fig. 2C). The hypertrophic zone was also slightly deformed in newborn mutant mice (Fig. 2C). Furthermore, the number and thickness of trabecular bones and the number of osteoblasts were significantly reduced in newborn *Cbfb^{fl/fl}Prx1-Cre* mice (Fig. 2D, E), the osteoclast number did not change (Fig. 2D-F). These results indicate that *Cbfb* is important for chondrocyte proliferation and maturation in newborn mice and that it may play a lesser role in osteoclasts.

Loss of *Cbfb* impaired growth plate development in P7 mice

Continuous postnatal skeletal development is required for normal development toward adulthood. H&E staining on paraffin sections of P7 mouse femur showed that growth plate and trabecular bone development were delayed in mutant mice (Fig. 3A, B). Comparable with the newborn mutant mice (Fig. 2B, C), P7 mutant mice also had shortened femurs, elongated growth plates, shortened diaphysis (Fig. 3A), elongated resting zones, and shortened and disorganized proliferation zones (Fig. 3B). While the hypertrophic zone was slightly deformed in newborn mutant mice (Fig. 2C), it was notably shortened in the P7 *Cbfb^{fl/fl}Prx1-Cre* mice (Fig. 3B). Moreover, proliferating cell nuclear antigen (PCNA) staining showed that the number of proliferating chondrocytes was decreased (Fig. 3C, D), and immunofluorescent (IF) staining showed that collagen type X (ColX) expression was reduced in mutant mice compared to WT (Fig. 3E). These results confirmed the retardation of chondrocyte proliferation and hypertrophy in *Cbfb^{fl/fl}Prx1-Cre* mice. Micromass culture of growth plate chondrocytes from newborn mice and Alcian blue staining confirmed that chondrocyte differentiation *in vitro* was also drastically delayed in the absence of *Cbfb* (Fig.

3F). Taken together, these results demonstrate that Cbfb plays important roles in growth plate formation in the early stages of postnatal development.

Loss of Cbfb blocked Ihh-cyclin D1 signalling and the Ihh-PTHrP negative feedback loop

Protein expression in the growth plates was detected by IF staining using P7 mouse femur sections (Fig. 4A-D, bright field views are co-presented in Supplementary Fig. S3A-D) and western blot using proteins from newborn mouse femoral cartilage (Fig. 4E, F). Expression of SRY-related high mobility group-Box gene 9 (Sox9), a key transcription factor in the chondrocyte lineage, was similar in WT and *Cbfb^{f/f}Prx1-Cre* mice (Figs. 4A; Supplementary Fig. S3A). However, expression of *Ihh* was dramatically reduced in *Cbfb^{f/f}Prx1-Cre* mice (Fig. 4B, E, F; Supplementary Fig. S3B). Cyclin D1, a cell-cycle-regulating protein downstream of *Ihh* (16), was also decreased in the proliferation zone of *Cbfb^{f/f}Prx1-Cre* femurs (Fig. 4C, E, F; Supplementary Fig. S3C), which may inhibit chondrocyte proliferation. Consistently, expression of other *Ihh* targeted genes besides Cyclin D1 [eg. *Pthlh* and *Patched (PTC)*] were also reduced in the growth plates of *Cbfb^{f/f}Prx1-Cre* mice. qRT-PCR using mRNA from newborn mouse femur showed that *Pthlh* expression was reduced by 30% in *Cbfb^{f/f}Prx1-Cre* mice (Supplementary Fig. S5B). IHC staining using P7 mouse femur sections showed that PTC expression was detected in the pre-hypertrophic zone in the growth plates in WT mice, but that it was greatly reduced in mutant mice (Fig. 4G). *Ihh* induces PTHrP expression in periarticular cells around pre-hypertrophic chondrocytes, which in turn suppresses chondrocyte differentiation through a feedback regulatory process denoted as the “*Ihh*-PTHrP negative feedback loop” (17). Interestingly, while *Ihh* and *Pthlh* expression were reduced, PPR expression was increased in the *Cbfb^{f/f}Prx1-Cre* growth plate. Up-regulation of PPR in *Cbfb^{f/f}Prx1-Cre* mice may increase the sensitivity of chondrocytes to PTHrP and retard chondrocyte hypertrophy even in the presence of a permissive dose of PTHrP resulting from decreased *Ihh* expression. In conclusion, *Cbfb* deficiency may affect chondrocyte proliferation by inhibiting *Ihh*-cyclin D1 signalling and interfere with normal chondrocyte hypertrophy by disturbing the *Ihh*-PTHrP negative feedback loop.

Runx/Cbfb complex regulated Ihh expression by binding to the *Ihh* promoter directly

In order to determine if the Runx/Cbfb complex binds the promoter region of *Ihh*, chromatin immunoprecipitation (ChIP) assay was performed using anti-Cbfb antibody and the primers shown in Fig. 5A. The ChIP input value using each primer pair represents the binding efficiency of its adjacent region. There were 16 predicted Runx-binding sites localizing in the *Ihh* promoter region (-3919/+27) (Fig. 4H). Primer pairs 4 and 5 resulted in the highest values (Fig. 4I), indicating that Runx2/Cbfb complex may bind sites 9-16 most efficiently. A 1.4-kb *Ihh* promoter region (-1287/+162), which contains Runx-binding sites 9-16, was cloned into the pGL3-basic vector. Luciferase activity driven by the *Ihh* promoter (-1287/+162) was low in the *Cbfb^{f/f}Prx1-Cre* chondrocytes and robustly increased (10-fold) after the expression of Cbfb (Fig. 4J). Ectopic expression of Runx2 further promoted the luciferase signal. In conclusion, we believe that the Runx/Cbfb heterodimer directly binds to the Runx-binding sites of the *Ihh* promoter regions and up-regulates *Ihh* expression at the transcriptional level.

Trabecular bone formation is impaired in MSC-specific *Cbfb*-deficient mice

Delayed ossification was observed in P1 (Supplementary Fig. S2D, E), P7 (Fig. 1), and 6-week-old (Fig. 2A) *Cbfb^{fl/fl}Prx1-Cre* mice. This was further confirmed by the H&E staining of P30 mice paraffin sections, which revealed a dramatic loss of trabecular bone in mutant mice (Fig. 5A, B). Notably, the growth plates were also severely deformed, protruding deep into the diaphysis (Fig. 5B, arrow). To investigate the potential role of *Cbfb* in osteoblasts *in vivo*, IF staining using mouse femur sections was performed (Fig. 5C-F; Supplementary Fig. S4). Expression of *Runx2* (a master transcription factor in the osteoblast lineage) was similar in P7 WT and *Cbfb^{fl/fl}Prx1-Cre* growth plates and trabecular bone, and increased in mutant perichondrium (Fig. 5E). Expression of *Runx3*, detected mainly in hypertrophic and pre-hypertrophic chondrocytes, was also similar between E18.5-day and E16.5-day WT and mutant femur (Supplementary Fig. S4). However, *Osx* (Osterix) (Fig. 5C) and *Opn* (Osteopontin) (Fig. 5D), which are osteoblast-related genes, showed reduced expression in P7 *Cbfb^{fl/fl}Prx1-Cre* trabecular bone compared with WT, indicating that osteoblastogenesis may be influenced. In addition, vascular endothelial growth factor (VEGF) expression was down-regulated in the growth plates of newborn mutant mice (Fig. 5F). Decreased VEGF expression results in reduced angiogenesis which may affect the population of MSC for normal trabecular bone formation. Taken together, these data demonstrate that *Cbfb* not only regulates chondrocyte proliferation and maturation, but that it also influences trabecular bone formation for normal skeleton morphogenesis.

Loss of *Cbfb* impaired osteoblastogenesis of calvarial cells *in vitro*

To further confirm the role of *Cbfb* in bone ossification, we investigated the role of *Cbfb* in osteoblastogenesis *in vitro* using osteoblast derived from calvarial cell primary culture (Fig. 6). Deletion of *Cbfb* expression in *Cbfb^{fl/fl}Prx1-Cre* osteoblasts was confirmed by quantitative RT-PCR (qRT-PCR) (Fig. 6C) and Western blot (Fig. 6G). *Cbfb^{fl/fl}Prx1-Cre* osteoblasts showed reduced alkaline phosphatase (ALP) activity (Fig. 6A) and mineralization (Fig. 6B) compared to WT cells, indicating that osteoblastogenesis was impeded in mutant cells. qRT-PCR revealed that the osteoclastogenesis related cytokines *receptor activator of nuclear factor- κ B ligand (RANKL)* was similarly expressed in *Cbfb^{fl/fl}Prx1-Cre* and WT osteoblasts (Fig. 6F). Expression of the osteoblast-related gene *Ocn* (*Osteocalcin*) was decreased in *Cbfb^{fl/fl}Prx1-Cre* cells on day 7 of osteoblastogenesis (Fig. 6D), and the expression of *Ocn*, *Opn*, *Alp* and *integrin binding sialoprotein (Ibsp)* was also decreased in *Cbfb^{fl/fl}Prx1-Cre* cells on day 14 of osteoblastogenesis (Fig. 6E, F). However, *Runx2* expression was increased (Fig. 6D, E), especially isoform 1 of *Runx2* (*Runx2-I*) (Fig. 6H). The expression of *Osx*, another master transcription factor of osteoblast differentiation, was also similar in WT and *Cbfb*-deficient cells (Fig. 6D, E). Considering that *Osx* expression was decreased in *Cbfb^{fl/fl}Prx1-Cre* trabecular bone (Fig. 5C), the mechanism by which *Runx2* regulates *Osx* expression may be different in calvaria and long bones. Western blot revealed that protein levels of *Runx2* and *Runx3* were not affected, but that expression of *Ocn* and *Runx1* was reduced in *Cbfb^{fl/fl}Prx1-Cre* osteoblasts on day 14 and 21 of osteoblastogenesis. When *Runx1* expression was selectively rescued in the endothelial and hematopoietic systems of *Runx1*^{-/-} embryos (*Runx1^{Re/Re}* mice), these mice survived until birth and displayed disrupted mineralization in some skull elements (6), indicating *Runx1*

play a role in calvarial osteoblastogenesis. Thus, Runx1 hypo-sufficiency in *Cbfb^{fl/fl}Prx1-Cre* cells may partially contribute to the impeded osteoblast differentiation. Taken together, these results indicate that Cbfb deficiency affects osteoblast differentiation *in vitro*.

Discussion

The Ihh-PTHrP negative feedback loop maintains chondrocyte proliferation and counters chondrocyte hypertrophy (17). We report that Cbfb plays a dual function in this loop by regulating the expression of Ihh and PPR (Fig. 4B, D), thereby affecting the balance of chondrocyte proliferation and maturation. The Runx/Cbfb complex binds the promoter region of the *Ihh* gene so as to regulate its expression (Fig. 5H-J). Consistently, diminished Ihh expression was also observed in *Runx2^{-/-}* and *Runx2^{-/-}Runx3^{-/-}* mice (4). It is therefore possible that Cbfb also regulates the Ihh-PTHrP negative feedback loop by interacting with Runx2 and Runx3, thereby regulating chondrocyte proliferation and maturation. Thus, Cbfb deficiency results in impaired growth plates development (Figs 2, 3) and severe skeletal malformation (Fig. 1).

Runx2 is a master regulator of the commitment and differentiation of pluripotent MSCs to osteoblasts (3). As a subunit of the CBF complex, Cbfb interacts with Runx2 to stabilize its interaction with DNA. pGL3-3XOSE2 was constructed by inserting three *OSE2* (18), a Runx2 binding sequence, into the pGL3-promoter. If only Runx2 and Cbfb were co-expressed, luciferase driven by the promoter with the *OSE2* sequence increased 1.7 folds (Supplementary Fig. S5A), indicating that Runx activities were deregulated in the *Cbfb*-deficient cells. Thus, *Cbfb^{fl/fl}Prx1-Cre* mice at birth displayed a similar, but less severe, phenotype to *Runx2^{-/-}* mice (3) (eg, reduced ossification and inhibited chondrocyte hypertrophy). Consistently, expression of Runx2 targeted genes, *ColX* (Fig. 3E) and *Ocn* (Fig. 6D, E), were also down-regulated in *Cbfb*-deficient mice. Although *Cbfb* has been reported to protect the Cbfa subunits from degradation (7), only Runx1 expression was reduced in *Cbfb^{fl/fl}Prx1-Cre* calvarial cells compared to WT (Fig. 6I), and Runx2 and Runx3 were similarly expressed in WT and *Cbfb^{fl/fl}Prx1-Cre* calvarial cells and long bones (Figs 6G, I, 5E; Supplementary Fig. S4). In fact, Runx2 expression was higher in *Cbfb^{fl/fl}Prx1-Cre* perichondrium compared to WT (Fig. 5E). Expression of *Runx2-I*, a specific *Runx2* isoform expressed in the perichondrium and proliferating chondrocytes (19), was also increased in *Cbfb^{fl/fl}Prx1-Cre* calvaria (Fig. 6H). Thus, the protection mechanism of Runx proteins may vary depending on the cell type and the differentiation stage. In addition, the high expression of Runx2 in the mutant mice where it would not normally have such high expression may indicate the immaturity of the cells.

While the *Runx2^{-/-}* skeletal system showed a complete lack of ossification (3), *Cbfb*-deficient mice only have delayed ossification. The delayed mineralization observed in the ribs and spines in some mice at birth became less severe as the mice aged. This indicates that Runx2 remains partially active without Cbfb. The *in vitro* promoter assay showed that the two isoforms of *Runx2* (i.e. *Runx2-I* and *Runx2-II*) retained some transcriptional activity in the absence of Cbfb (13). qRT-PCR showed that *Runx2-I* expression was increased in *Cbfb*-deficient calvaria (Fig. 6H). The partially rescued phenotype of *Cbfb*-deficient mice may be a combined action of the remaining activity of Runx2-I and Runx2-II.

Cbfb β may form a complex with Runx2 or Runx3 to regulate Ihh expression, and thereby regulate chondrocyte proliferation and maturation. Recent studies have shown that the Cbfb β /Runx1 complex plays an important role in chondrogenesis and chondrocyte proliferation (20). Soung *et al.* reported that Runx1 is required for endochondral ossification during skeletal development (21). Moreover, Runx1 and Cbfb β both have much higher expression levels in MSCs and chondrocytes than Runx2 and Runx3 do (21). In addition, Runx2 is usually considered as a positive regulator in chondrocyte maturation rather than in chondrocyte proliferation (22,23). All these studies indicate that the Runx1/Cbfb β complex may exert a more important role than Runx2/Cbfb β and Runx3/Cbfb β in chondrocyte proliferation. To our knowledge, our study is the first report of Cbfb β regulating chondrocyte proliferation. Additional studies are needed to characterize the mechanism underlying the roles of Runx/Cbfb β complexes in regulating the chondrocyte proliferation *in vivo*.

In summary, we investigated the role of Cbfb β in postnatal cartilage and bone development. We found that Cbfb β is a key factor for chondrocyte proliferation, chondrocyte differentiation, and the maintenance of growth plates and trabecular bone in postnatal mice. Cbfb β up-regulated Ihh and down-regulated PPR in postnatal growth plates and thereby controlled the proliferation of chondrocytes to pre-hypertrophic chondrocytes. Our results also indicate that Cbfb β may interact with Runx1 to regulate chondrocyte proliferation.

Supplementary Material

Refer to Web version on PubMed Central for supplementary material.

Acknowledgements

We would like to thank Mr. Matthew McConnell and Dr. Joel Jules for their extensive reading, discussion, and excellent assistance with this manuscript. We thank Ms. Christie Paulson for her excellent assistance with the manuscript. We thank Mr. Matthew McConnell for his excellent assistance with bioinformatics work and ChIP primer design. We appreciate the assistance of the Center for Metabolic Bone Disease at the University of Alabama at Birmingham (UAB) (P30 AR046031). We are also grateful for the assistance of the Small Animal Phenotyping Core, Metabolism Core, and Neuroscience Molecular Detection Core Laboratory at UAB (P30 NS0474666). This work was supported by NIH grants AR-055307 (Y.P.L.) and R01-AR-44741 (Y.P.L.).

References

1. Speck NA, Terry S. A new transcription factor family associated with human leukemias. *Crit Rev Eukaryot Gene Expr.* 1995; 5(3-4):337–64. [PubMed: 8834230]
2. Levanon D, Negreanu V, Bernstein Y, Bar-Am I, Avivi L, Groner Y. AML1, AML2, and AML3, the human members of the runt domain gene-family: cDNA structure, expression, and chromosomal localization. *Genomics.* 1994; 23(2):425–32. [PubMed: 7835892]
3. Komori T, Yagi H, Nomura S, Yamaguchi A, Sasaki K, Deguchi K, Shimizu Y, Bronson RT, Gao YH, Inada M, Sato M, Okamoto R, Kitamura Y, Yoshiki S, Kishimoto T. Targeted disruption of Cbfa1 results in a complete lack of bone formation owing to maturational arrest of osteoblasts. *Cell.* 1997; 89(5):755–764. [PubMed: 9182763]
4. Yoshida CA, Yamamoto H, Fujita T, Furuichi T, Ito K, Inoue K, Yamana K, Zanma A, Takada K, Ito Y, Komori T. Runx2 and Runx3 are essential for chondrocyte maturation, and Runx2 regulates limb growth through induction of Indian hedgehog. *Genes Dev.* 2004; 18(8):952–63. [PubMed: 15107406]
5. Kimura A, Inose H, Yano F, Fujita K, Ikeda T, Sato S, Iwasaki M, Jinno T, Ae K, Fukumoto S, Takeuchi Y, Itoh H, Imamura T, Kawaguchi H, Chung UI, Martin JF, Iseki S, Shinomiya K, Takeda

- S. Runx1 and Runx2 cooperate during sternal morphogenesis. *Development*. 2010; 137(7):1159–67. [PubMed: 20181744]
6. Liakhovitskaia A, Lana-Elola E, Stamateris E, Rice DP, van 't Hof RJ, Medvinsky A. The essential requirement for Runx1 in the development of the sternum. *Dev Biol*. 2010; 340(2):539–46. [PubMed: 20152828]
 7. Huang G, Shigesada K, Ito K, Wee HJ, Yokomizo T, Ito Y. Dimerization with PEBP2beta protects RUNX1/AML1 from ubiquitin-proteasome-mediated degradation. *EMBO J*. 2001; 20(4):723–33. [PubMed: 11179217]
 8. Sasaki K, Yagi H, Bronson RT, Tominaga K, Matsunashi T, Deguchi K, Tani Y, Kishimoto T, Komori T. Absence of fetal liver hematopoiesis in mice deficient in transcriptional coactivator core binding factor beta. *Proc Natl Acad Sci U S A*. 1996; 93(22):12359–63. [PubMed: 8901586]
 9. Wang Q, Stacy T, Miller JD, Lewis AF, Gu TL, Huang X, Bushweller JH, Bories JC, Alt FW, Ryan G, Liu PP, Wynshaw-Boris A, Binder M, Marin-Padilla M, Sharpe AH, Speck NA. The CBFbeta subunit is essential for CBFalpha2 (AML1) function in vivo. *Cell*. 1996; 87(4):697–708. [PubMed: 8929538]
 10. Kundu M, Javed A, Jeon JP, Horner A, Shum L, Eckhaus M, Muenke M, Lian JB, Yang Y, Nuckolls GH, Stein GS, Liu PP. Cbfbeta interacts with Runx2 and has a critical role in bone development. *Nat Genet*. 2002; 32(4):639–44. [PubMed: 12434156]
 11. Miller J, Horner A, Stacy T, Lowrey C, Lian JB, Stein G, Nuckolls GH, Speck NA. The core-binding factor beta subunit is required for bone formation and hematopoietic maturation. *Nat Genet*. 2002; 32(4):645–9. [PubMed: 12434155]
 12. Yoshida CA, Furuichi T, Fujita T, Fukuyama R, Kanatani N, Kobayashi S, Satake M, Takada K, Komori T. Core-binding factor beta interacts with Runx2 and is required for skeletal development. *Nat Genet*. 2002; 32(4):633–8. [PubMed: 12434152]
 13. Kanatani N, Fujita T, Fukuyama R, Liu W, Yoshida CA, Moriishi T, Yamana K, Miyazaki T, Toyosawa S, Komori T. Cbf beta regulates Runx2 function isoform-dependently in postnatal bone development. *Dev Biol*. 2006; 296(1):48–61. [PubMed: 16797526]
 14. Naoe Y, Setoguchi R, Akiyama K, Muroi S, Kuroda M, Hatam F, Littman DR, Taniuchi I. Repression of interleukin-4 in T helper type 1 cells by Runx/Cbf beta binding to the Il4 silencer. *J Exp Med*. 2007; 204(8):1749–55. [PubMed: 17646405]
 15. Logan M, Martin JF, Nagy A, Lobe C, Olson EN, Tabin CJ. Expression of Cre Recombinase in the developing mouse limb bud driven by a Prxl enhancer. *Genesis*. 2002; 33(2):77–80. [PubMed: 12112875]
 16. Long F, Zhang XM, Karp S, Yang Y, McMahon AP. Genetic manipulation of hedgehog signaling in the endochondral skeleton reveals a direct role in the regulation of chondrocyte proliferation. *Development*. 2001; 128(24):5099–108. [PubMed: 11748145]
 17. Kronenberg HM. Developmental regulation of the growth plate. *Nature*. 2003; 423(6937):332–6. [PubMed: 12748651]
 18. Ducy P, Karsenty G. Two distinct osteoblast-specific cis-acting elements control expression of a mouse osteocalcin gene. *Mol Cell Biol*. 1995; 15(4):1858–69. [PubMed: 7891679]
 19. Xiao ZS, Hjelmeland AB, Quarles LD. Selective deficiency of the “bone-related” Runx2-II unexpectedly preserves osteoblast-mediated skeletogenesis. *J Biol Chem*. 2004; 279(19):20307–13. [PubMed: 15007057]
 20. Johnson K, Zhu S, Tremblay MS, Payette JN, Wang J, Bouchez LC, Meeusen S, Althage A, Cho CY, Wu X, Schultz PG. A stem cell-based approach to cartilage repair. *Science*. 2012; 336(6082):717–21. [PubMed: 22491093]
 21. Soung do Y, Talebian L, Matheny CJ, Guzzo R, Speck ME, Lieberman JR, Speck NA, Drissi H. Runx1 dose-dependently regulates endochondral ossification during skeletal development and fracture healing. *J Bone Miner Res*. 2012; 27(7):1585–97. [PubMed: 22431360]
 22. Enomoto H, Enomoto-Iwamoto M, Iwamoto M, Nomura S, Himeno M, Kitamura Y, Kishimoto T, Komori T. Cbfa1 is a positive regulatory factor in chondrocyte maturation. *J Biol Chem*. 2000; 275(12):8695–702. [PubMed: 10722711]
 23. Drissi MH, Li X, Sheu TJ, Zuscik MJ, Schwarz EM, Puzas JE, Rosier RN, O'Keefe RJ. Runx2/Cbfa1 stimulation by retinoic acid is potentiated by BMP2 signaling through interaction with

Smad1 on the collagen X promoter in chondrocytes. *J Cell Biochem.* 2003; 90(6):1287–98.
[PubMed: 14635200]

Author Manuscript

Author Manuscript

Author Manuscript

Author Manuscript

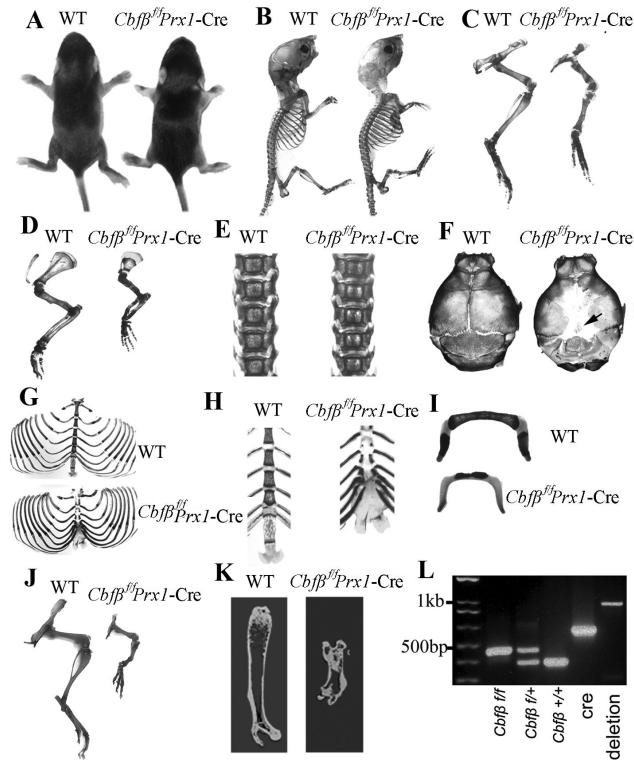


Fig. 1. *Cbfb^{f/f}Prx1-Cre* mice had dwarfism with shortened limbs

(A) Gross morphology of postnatal 7-day-old (P7) *Cbfb^{f/f}Prx1-Cre* and wild-type (WT) mice. (B-I) Skeletal analysis by Alizarin red S/Alcian blue staining of P7 *Cbfb^{f/f}Prx1-Cre* and WT mice. Long bones were shorter (C,D), sutures and fontanelles were widened (black arrow) (F), and ossification of parietal bones (F), frontal bone (F), sternum (H) and hyoid bone (I) was delayed in *Cbfb^{f/f}Prx1-Cre* mice. Development of ribs (G) and spine (E) was not affected in *Cbfb^{f/f}Prx1-Cre* mice. (J) Skeletal analysis by Alizarin red S/Alcian blue staining of P30 *Cbfb^{f/f}Prx1-Cre* and WT mouse limb. (K) Micro-CT analysis of P30 *Cbfb^{f/f}Prx1-Cre* and WT mouse femur. (L) PCR was used to determine *Cbfb* alleles (*f/f*, *f/+*, *+/+*, or deletion) and the presence of Cre.

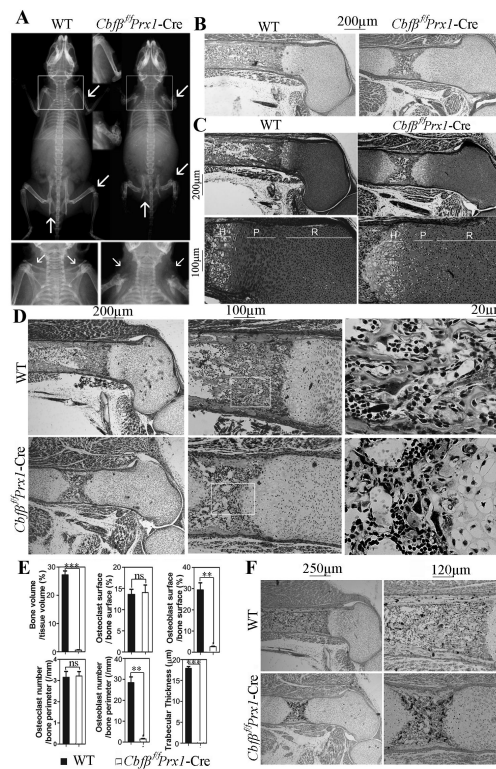


Fig. 2. *Cbfb* deficiency resulted in cleidocranial dysplasia-like phenotype in adult mice and skeletal defects in newborn mice

(A) Whole body X-ray of 6-week-old mice showed cleidocranial dysplasia-like phenotype of *Cbfb^{fl/fl}Prx1-Cre* mice, including shortened stature, shortened long bones (upper lane, marked by arrowhead), and absent clavicles (lower lane marked by arrowhead and upper lane marked by arrowhead and square). (B) H&E staining of paraffin sections of femurs from newborn *Cbfb^{fl/fl}Prx1-Cre* mice and WT mice. (C) Safranin O staining of paraffin sections of femurs from newborn *Cbfb^{fl/fl}Prx1-Cre* mice and WT mice. (D) Goldner's trichrome staining of paraffin sections of femurs from newborn *Cbfb^{fl/fl}Prx1-Cre* mice and WT mice. (E) Quantification data of Goldner's trichrome staining were presented as mean \pm SD, $n \geq 6$, ns (non-significant), $**p < 0.01$, $***p < 0.001$ versus WT. (F) TRAP staining of paraffin sections of femurs from newborn *Cbfb^{fl/fl}Prx1-Cre* mice and WT mice. P: proliferation zone. R: resting zone. H: hypertrophic zone.

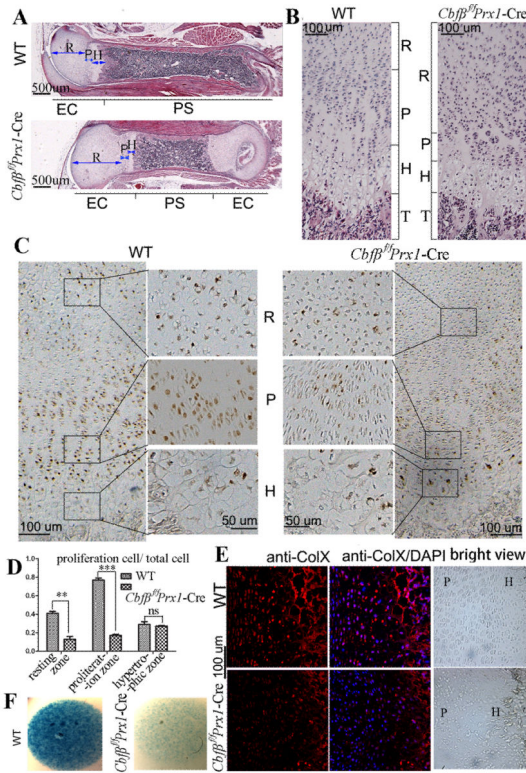


Fig. 3. *Cbfb* deficiency retards the development of primary spongiosa and delays chondrocyte proliferation and maturation

(A, B) H&E staining of paraffin sections of femurs from P7 *Cbfb^{fl/fl}Prx1-Cre* mice and WT mice. Femur and primary spongiosa were shortened, while the epiphyseal growth plate was elongated in *Cbfb^{fl/fl}Prx1-Cre* mice. Columnar structure of proliferative chondrocyte zone was lost in *Cbfb^{fl/fl}Prx1-Cre* mice. (C) PCNA staining of paraffin sections of femurs from P7 *Cbfb^{fl/fl}Prx1-Cre* mice and WT mice. Second and third columns show magnified images of areas in black boxes. (D) The ratio of proliferating cells in total cells in the three chondrocyte zones of WT and *Cbfb^{fl/fl}Prx1-Cre* mice from (C). Data were presented as mean \pm SD, $n \geq 6$, ns (non-significant), ** $p < 0.01$, *** $p < 0.001$ versus the same zone in WT mice. (E) IF staining using frozen sections of P7 mouse femurs showed that ColX expression was decreased in *Cbfb^{fl/fl}Prx1-Cre* mice. Bright field views were co-presented on the right panel. (F) Micromass culture of growth plate chondrocytes of newborn mice. PS: primary spongiosa. EC: epiphyseal cartilage. R: resting zone. P: proliferation zone. H: hypertrophic zone. T: trabecular bone.

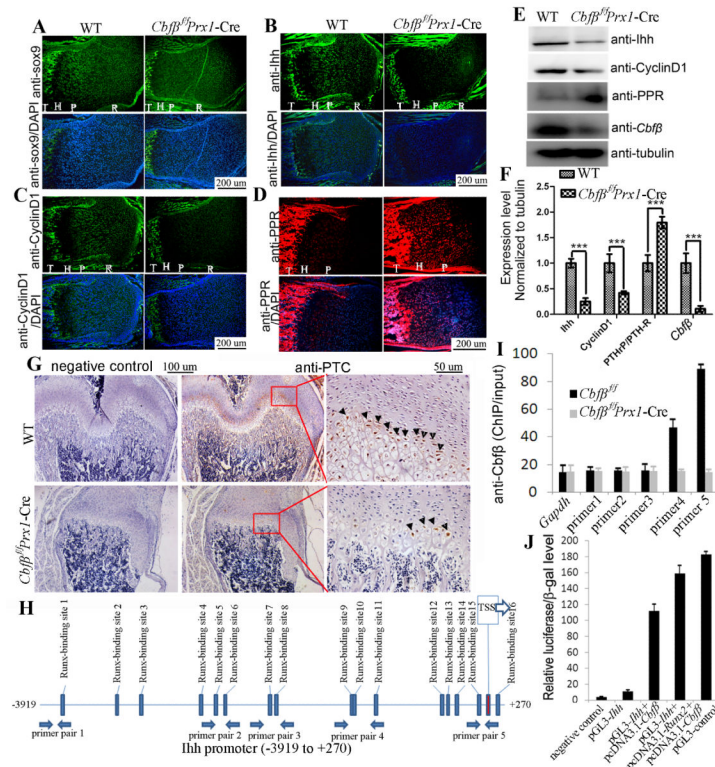


Fig. 4. Expression of Sox9, Ihh, CyclinD1, PTHrP-R, and Cbfb in chondrocytes of *Cbfb^{f/f}Prx1-Cre* mice and WT mice

Similar Sox9 expression (A), decreased Ihh expression (B), decreased Cyclin D1 expression (C), and increased PPR expression (D) was observed in femur growth plates of P7 *Cbfb^{f/f}Prx1-Cre* mice compared to that of WT mice, as detected by IF staining using frozen sections. (E) The expression of Ihh, CyclinD1, PPR and Cbfb was confirmed by Western blot using protein lysates of femoral cartilage from *Cbfb^{f/f}Prx1-Cre* and WT newborn mice. (F) Protein levels in (E) were quantified and normalized to tubulin. (G) The expression of Patched (PTC) in the pre-hypertrophic zone of the growth plates in P7 *Cbfb^{f/f}Prx1-Cre* mice was reduced compared with that in WT mice, as detected by IHC staining using paraffin sections. Third column shows the magnified images of areas in red boxes. Arrowheads indicate positive stains. R: resting zone. P: proliferation zone. H: hypertrophic zone. T: trabecular bone. (H) Schematic display of the *Ihh* promoter region (-3919/+270). TSS (transcriptional start site), predicted Runx-binding sites and ChIP primer positions were indicated in the figure. (I) ChIP was performed using WT chondrocyte lysates, anti-Cbfb antibody, and primers as indicated in (H). (J) The *Ihh* promoter region (-1287/+162) was inserted into the pGL3-basic vector. Primary *Cbfb^{f/f}Prx1-Cre* chondrocytes were transfected with pGL3-control, pGL3-*Ihh*+pcDNA3.1a-*Cbfb*, or pGL3-*Ihh*+pcDNA3.1a-*Cbfb*+pcDNA3.1a-*Runx2*. The β-GAL-expression plasmid was also co-transfected. Luciferase activity was detected 48 hours post-transfection, and normalized to β-GAL activity. Data were presented as mean ± SD, n ≥ 6, ns (non-significant), ***p < 0.001.

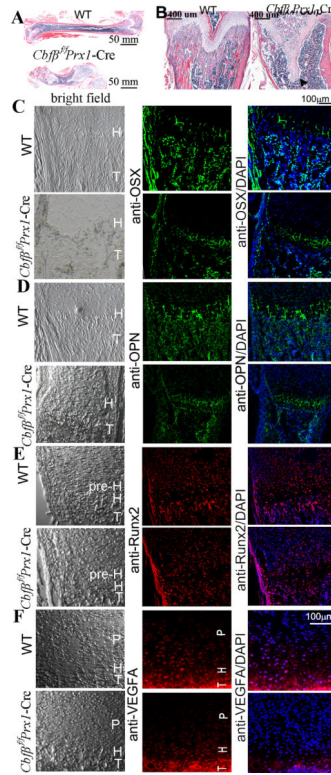


Fig. 5. Mice lacking *Cbfb* had delayed ossification

(A,B) H&E staining of the femurs of P30 (postnatal one-month-old) WT and *Cbfb^{fl/fl}Prx1-Cre* mice. The femur was shortened and trabecular bone was lost in *Cbfb^{fl/fl}Prx1-Cre* mice. The epiphyseal growth plate protruded deep into the diaphysis abnormally (marked by arrowhead). (C-F) IF staining using frozen sections of femurs of P7 (C-E) and newborn (F) WT and *Cbfb^{fl/fl}Prx1-Cre* mice. In the *Cbfb^{fl/fl}Prx1-Cre* mice, expression of OSX (C), OPN (D) and VEGFA (F) was decreased, but expression of Runx2 (E) was not changed. Bright field views of C-F are co-presented on the left panel. T: trabecular bone. H: hypertrophic zone. P: proliferation zone. pre-H: pre-hypertrophic zone.

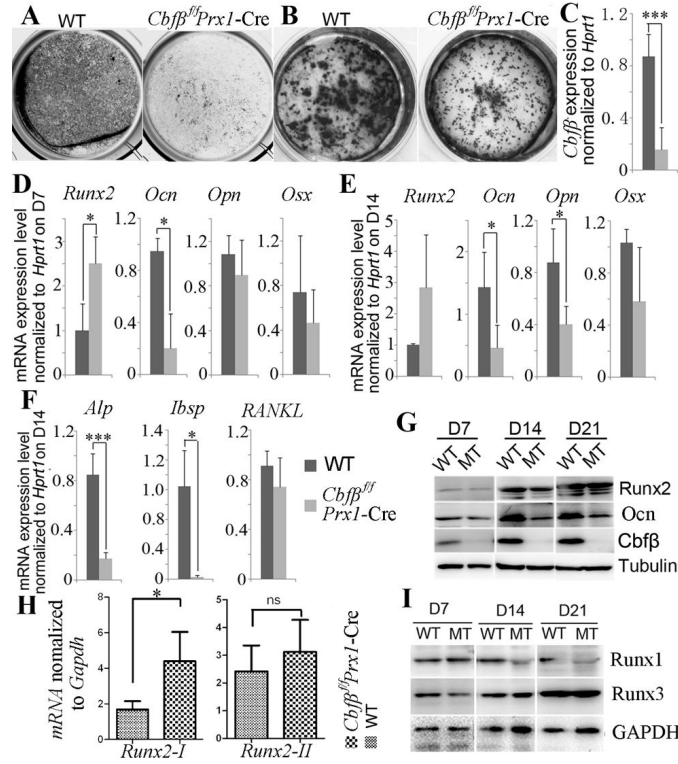


Fig. 6. Cbfb is required for osteoblastogenesis of calvarial cells

Calvarial cells from *Cbfb^{fl/fl}Prx1-Cre* and WT newborn mice were used for primary culture. Osteoblastogenesis was detected by (A) ALP staining on day 14 of osteoblastogenesis and mineralization was detected by (B) Von Kossa staining on day 21 of osteoblastogenesis. (C) *Cbfb* expression levels in calvarial cells were detected by qRT-PCR and normalized to *Hprt1*. (D, E) Expression of *Runx2*, *Opn*, *Ocn*, and *Osx* in calvarial cells on day 7 (D7) (D) and day 14 (D14) (E) of osteoblastogenesis was detected by qRT-PCR and normalized to *Hprt1*. (F) Expression of *Alpl*, *Ibsp* and *RANKL* in calvarial cells on day 14 of osteoblastogenesis was detected qRT-PCR and normalized to *Hprt1*. (G) Western blot was applied to detect the protein levels of Runx2, Ocn, and Cbfb in WT and mutant (MT) calvarial cells on day 7, 14, and 21 (D7, D14 and D21) of osteoblastogenesis. (H) Expression levels of *Runx2-I* and *Runx2-II* in calvaria were determined by qRT-PCR and normalized to *Gapdh*. (I) Western blot was applied to detect the protein levels of Runx1 and Runx3 in WT and mutant calvarial cells on day 7, 14, and 21 of osteoblastogenesis. Results were presented as mean ± SD, n ≥ 6, ns (non-significant), *p < 0.05, ***p < 0.005.